Physica A 488 (2017) 1–7

Contents lists available at ScienceDirect

Physica A

journal homepage: www.elsevier.com/locate/physa

Hurst exponent: A Brownian approach to characterize the nonlinear behavior of red blood cells deformability

M.A. Mancilla Canales [a,*], A.J. Leguto [a,e], B.D. Riquelme [c], P. Ponce de León [b], S.A. Bortolato [a,d], A.M. Korol [a,c]

[a] Department of Mathematics and Statistics, National University of Rosario, Suipacha 531, 2000 Rosario, Argentina
[b] Department of Parasitology, , National University of Rosario, Suipacha 531, 2000 Rosario, Argentina
[c] Institute of Physics Rosario (IFIR-CONICET), Ocampo 210bis, 2000 Rosario, Argentina
[d] Institute of Chemistry Rosario (IQUIR-CONICET), Suipacha 570, 2000 Rosario, Argentina
[e] Institute of Molecular and Cell Biology Rosario (IBR CONICET), Ocampo 210bis, 2000 Rosario, Argentina

ARTICLE INFO

Article history:
Received 13 April 2017
Available online 8 July 2017

Keywords:
Nonlinear quantifiers
Hurst exponent
Ektacytometry
Erythrocytes
Fractals

ABSTRACT

Ektacytometry techniques quantifies red blood cells (RBCs) deformability by measuring the elongation of suspended RBCs subjected to shear stress. Raw shear stress elongation plots are difficult to understand, thus most research papers apply data reduction methods characterizing the relationship between curve fitting. Our approach works with the naturally generated photometrically recorded time series of the diffraction pattern of several million of RBCs subjected to shear stress, and applies nonlinear quantifiers to study the fluctuations of these elongations. The development of new quantitative methods is crucial for restricting the subjectivity in the study of the cells behavior, mainly if they are capable of analyze at the same time biological and mechanical aspects of the cells in flowing conditions and compare their dynamics. A patented optical system called Erythrocyte Rheometer was used to evaluate viscoelastic properties of erythrocytes by Ektacytometry. To analyze cell dynamics we used the technique of Time Delay Coordinates, False Nearest Neighbors, the forecasting procedure proposed by Sugihara and May, and Hurst exponent. The results have expressive meaning on comparing healthy samples with parasite treated samples, suggesting that apparent noise associated with deterministic chaos can be used not only to distinguish but also to characterize biological and mechanical aspects of cells at the same time in flowing conditions.

1. Introduction

On healthy individuals as well as on patients affected by *Ascaris lumbricoides* (AL) parasites, their red blood cells (RBCs) are forced to travel along capillaries of the microcirculation with diameters smaller than the cells themselves. This requires significant cellular deformability and this viscoelastic property is known to be impaired in several hematological diseases. Reduced ability of RBCs to change shape under these conditions may prompt microcirculatory dysfunction thus aggravating the clinical symptoms [1–5].

A previous *in vitro* study of the influence of AL on rheological nonlinear parameters was carried out by incubating normal erythrocytes at different larvae and parasite extract concentrations. And it was found that washed erythrocytes from healthy individuals incubated with high parasite level concentrations showed both increased levels of cell agglutination and

* Corresponding author.
E-mail address: mmancill@fbioyf.unr.edu.ar (M.A. Mancilla Canales).

http://dx.doi.org/10.1016/j.physa.2017.06.009
0378-4371/

decreased values of erythrocyte filterability [6–8]. Also, our preliminary study on RBCs complex behavior, when they are incubated with AL larvae, have shown the suitability of box-counting method to measure fractal dimension of erythrocytes images when trying to characterize the different populations by image analysis [9].

In order to further study the manifestation of the complex behavior related to RBCs could be applied other concepts. The techniques of Time Delay Coordinates suggested by Takens, False Nearest Neighbors proposed by Abarbanel and co-workers [10] and the method proposed by Sugihara and May [11]. The latter provides an estimation of the number of degrees of freedom, and also makes inferences about the dynamical nature of the system under study. This inference can be carried out by examining the correlation coefficient between predicted and observed time series through different prediction intervals, depending on the embedding dimension of the attractor as long as the photometric time series is identified as chaotic. Finally, Hurst exponent would allow to characterize ordinary Brownian motion and fractional Brownian motion not only for photometrically recorded series but also for shuffle surrogates obtained from the experimental ones.

The forecasting techniques discussed here are phenomenological in the sense that they attempt to evaluate the dynamic evolution of the system and to make short range predictions based on that evaluation.

The aim of our work was to detect possible changes between viscoelastic properties behavior of RBCs incubated with adult AL extracts and of control RBCs populations by analyzing one dimensional photometrically recorded time series of cells under shear stress. The time series were obtained by Ektacytometry technique using a device developed and patented by our Group of Applied Optics at Biology from IFIR (CONICET-UNR) [12].

2. Materials and methods

2.1. Samples preparation of RBCs

Human venous blood samples of red cells Group 0 were anticoagulated with Na_2EDTA and maintained at 4 °C until they were processed. Whole blood was centrifuged at 800 g during 10 min. Then, plasma and buffer coat were removed. The remaining RBCs were washed three times with phosphate buffer saline (PBS, pH 7.4) at 25 °C.

Erythrocyte suspensions were obtained according to the experimental procedure described above and following the International Committee for Standardization on Hematology [13]. Erythrocyte osmotic resistance, viscoelastic parameters, increase in fragility and rheological alterations of RBCs with adult AL extracts were measured as explained in previous work [12].

We worked with adult AL extracts following the protocol description given in Ref. [9]. The incubation procedure was made with washed RBCs and extract of parasites both at the same volume during 30 min at 37 °C.

2.2. Data acquisition

The Erythrocyte Rheometer based on Ektacytometry, was used to data acquisition [14,15]. In this instrument, light diffraction under Fraunhofer theory conditions may be applied to obtain quantitative information of diffracting particles such as suspended RBCs. Cells in dilute suspension under shear stress take a three axial ellipsoidal shape having the major axis in the same direction towards the shear field direction. A laser beam that transverse perpendicularly a thin layer of cells suspension is diffracted producing a Fraunhofer diffraction pattern that is either circular when the cells are at rest or elliptical when they become deformed by a shear stress field [16,17].

Normal RBCs being at rest can be considered as a monodisperse population having discoid shapes with almost the same size. RBCs suspension is placed between two flint glass disks, and a driving motor allows the rotation of the lower disk. Data is stored for being numerically processing. Based on previous reports, the time series obtained were split in two parts: the first one describes the stage when the erythrocytes are subjected to shear stress and the second one describes the stage when the erythrocytes recover their circular shape for being at rest [18–20].

An example of the time series for the creep process and for a healthy control sample obtained by the equipment, as well as the Fraunhofer diffraction patterns for rest and under shear stress, is shown in Fig. 1.

3. Data analysis

3.1. Shuffle surrogate data

We applied the random shuffle surrogate procedure to all the recorded time series in order to investigate irregular fluctuations and to be able to analyze whether the data can be fully described by independent and identically distributed random variables with no periodicities. With this procedure, it is possible to destroy local structures on short term variability and to preserve the global behaviors.

An important role of surrogates is being a numerical control of the results obtained for the photometrically time series [21]. In order to obtain a shuffle surrogate from our recorded time series of red blood cells subjected to well controlled shear stress; we divided the series in 100 parts. All the time series of 3500 data points where divided in 100 series of 35 data points each. Then these shorter series were concatenated at random to generate new and different time series of 3500

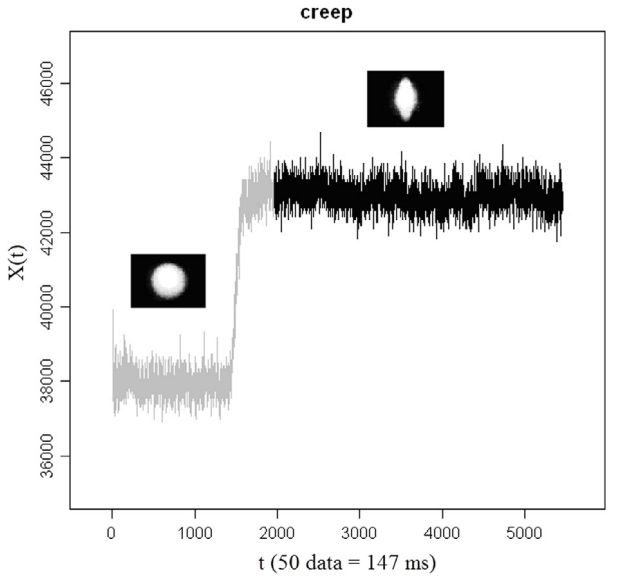

Fig. 1. Typical time series from the creep process of erythrocytes under shear stress and Fraunhofer diffraction patterns for rest and under shear stress.

data points. Surrogates obtained in this way may seem trivial, but it is a good way to verify that some specific aspect of the distribution of values in the signal is not fooling the correlation coefficient algorithm.

The null hypothesis is that the measured signal is a set of values drawn from a finite population without apparent order. On our hypotheses, despite the surrogates have been generated obtaining completely different time series, all of them share the power spectrum with the original one.

3.2. The percentage of false nearest neighbors

A particular time series, such as the data set depicted in Fig. 1, can be connected in time, leading to an orbit or trajectory that represents the evolution of the system. The set of orbits starting from all possible initial conditions generates a flow in the state space and can be used to visualize the attractor of the system. However, limitations of such representation of the system include the conditions that every trajectory must be non-intersecting and that different trajectories originating from different initial conditions must not overlap or occupy the same space. This arises from the fact that a point in phase space representing the state of the system is considered to encode all the information about the system, including both its past and future history, which in a deterministic system must be unique.

In this phase space, points of an orbit acquire neighbors. These neighbors provide information on how phase space neighborhoods evolve in time. In an embedding dimension E, that is too small to unfold the attractor, not all the points that are close to each other will be actually neighbors due to the dynamics. Some of them will be far from each other, and simply appear as neighbors because the geometric structure of the attractor has been projected onto a smaller space.

Abarbanel and co-workers [10] evaluated neighbors with increasing dimensions until no false neighbors remained. They developed a specifically method from geometrical considerations, known as percentage of false nearest neighbors (%FNN). The proposed method looks for a value for the minimum embedding dimension that correctly analyze the dynamics of the process.

In D dimension each vector $Y(k)$ will have a nearest neighbor $Y_{NN}(k)$, in the sense of the minimum Euclidean distance between them:

$$R_D^2(k) = |Y(k) - Y_{NN}(k)|^2 = \sum_{j=0}^{D-1} (y(k - j\tau) - y_{NN}(k - j\tau))^2 \tag{1}$$

$$\begin{aligned} R_{D+1}^2(k) &= |Y(k) - Y_{NN}(k)|^2 = \sum_{j=0}^{D} (y(k - j\tau) - y_{NN}(k - j\tau))^2 \\ &= \sum_{j=0}^{D-1} (y(k - j\tau) - y_{NN}(k - j\tau))^2 + (y(-D\tau) + y_{NN}(k - D\tau))^2 \\ &= R_D^2(k) + (y(-D\tau) + y_{NN}(k - D\tau))^2. \end{aligned} \tag{2}$$

From Eqs. (1)–(2), if R_D is the minimum distance between $Y(k)$ and $Y_{NN}(k)$, then R_{D+1} must be smaller than R_D, but if it is bigger, then the attractor in R_D is not unfolded and those points appeared near because the real attractor has been projected on a smallest space on delay coordinates.

This could be checked for increasing embedding dimensions until %FNN is less than 1%. The calculation of the %FNN could be used as a test on measurements from dynamical system in order to find the minimum embedding dimension E in which the attractor of the system is completely unfolded.

3.3. Sugihara and May correlation coefficient

Specifically, we first choose the smallest embedding dimension E in which every trajectory must be non-intersecting, as obtained with the %FNN procedure. We used the technique of time delay coordinates suggested by Takens and co-workers [22] in order to generate the phase space portraiture for the systems dynamics.

A convenient way to reconstruct the dynamics of the process is to unfold the time series by successively higher shifts. The shifts were defined as integer multiples of a fixed lag $\boldsymbol{\tau}$, where $\boldsymbol{\tau}$ is an integer number defined as $\boldsymbol{\tau} = m\Delta t$ (in our work, $m = 1$). Taking $\mathbf{N}$ equidistant points for creep and recovery process, we are able to define the phase space of all the possible states of the system variables under study.

For our time series, each sequence for which we wish to make a prediction is now to be regarded as an E-dimensional point, that is a vector, comprising the present value and the $E - 1$ previous values each separated by one lag time.

We now place all nearby E-dimensional points in the state space as proposed by May and Sugihara [11]. For each of these points a minimal neighborhood is defined to be such that the predicted one (Y^*) is contained within the smallest simplex. A simplex containing $E + 1$ vertices is the smallest simplex that can contain an E-dimensional point as an inside one. The lower dimensional simplex of nearest neighbors was used for points on the boundary.

Prediction is now obtained by projecting the domain of the simplex into its range, which is done by keeping track of where the points in the simplex end up after $\boldsymbol{s}$ time steps. To obtain the predicted value, we compute where the original predicted one has moved within the range of this simplex. This is a nonparametric method, which uses no prior information about the model used to generate the series; the only information is the output itself. It should apply to any stationary or quasi ergodic dynamic process, including chaos.

When plotting the conventional statistical coefficient correlation $\langle C_s(Y, Y^*)\rangle$ between predicted Y^* and observed values Y as a function of $\boldsymbol{s}$, if one obtains a decrease in the correlation coefficients with increasing prediction time then this is a characteristic feature of chaos [11]. This property is noteworthy because it indicates a simple way to differentiate additive noise from deterministic chaos. The former is uncorrelated, regardless of how far or close into the future one tries to project the simplex, whereas predictions with the latter will tend to deteriorate as one tries to forecast further into the future.

Our predictions were generated by using the first half of the data series to construct an ensemble of points in an E-dimensional state space. This first half was the library of past patterns; they were done avoiding the first 500 data points corresponding to the stationary process. Then the resulting information was used to depict the remaining second half values in the series. This collection of information has been little analyzed when studying erythrocytes viscoelasticity and, for our best knowledge, not at all in the light of contemporary notions about nonlinear dynamics.

3.4. Random walk approach: Brownian motion and Hurst exponent

In this approach for ordinary and fractional Brownian motion, the recorded time series corresponding to the long axes of the diffraction pattern of the cells when undergo shear stress were studied from nonlinear correlation to Hurst exponents.

In a classical non differentiable trajectory or, more generally, ordinary Brownian motion (OBM), past increments in displacement are uncorrelated with future increments, that is, the system has no memory. In a correlated random walk, or more generally, fractional Brownian motion (FBM), past increments in displacement are correlated with future increments, at least for the first steps of the process, hence the system has memory.

Hurst exponent for a time series provides a measure of whether it is a pure white noise random process or has underlying trends. Dynamic process, that might naively characterized with purely white noise, sometimes turn out to exhibit Hurst exponent statistics for long memory process, i.e., colored noise. A long memory process is a process where past events have a decaying effect on future ones. But those are forgotten as time moves forward.

A time dependent function $X(t)$, as ours photometrically recorded time series, is said to be self-affine if fluctuations in different scales can be rescaled in order to obtained the original signal, to be statistical equivalent to the rescaled version [23].

$$X(t) = \lambda^{-H} x(\lambda t). \tag{3}$$

In Eq. (3), λ is a positive number and H is the Hurst exponent, which quantifies the degree of correlation (positive or negative) when the increments are $\Delta Y(t_i) = y(t_{i+1}) - y(t_i)$.

It can be shown that for a process satisfying the self-affine property, the correlation function $\langle C_s(Y, Y^*)\rangle$ between $\Delta Y(t)$ of the real series and $\Delta Y^*(t)$ for the predicted one, can be best illustrated by considering the correlation coefficient for Brownian motion, proposed by Feder [24], which is given by the expression:

$$C(t) = \frac{\langle \Delta Y(t)\, \Delta Y^*(t)\rangle}{\langle [\Delta Y(t)]^2\rangle} = 2^{2H-1} - 1. \tag{4}$$

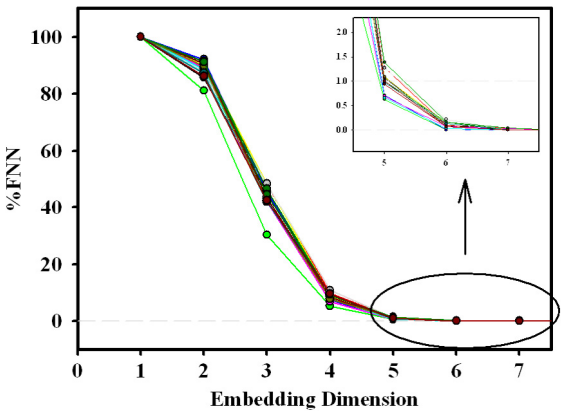

Fig. 2. Embedding dimension E vs. %FNN.

From Eq. (4), if $H = 0.5$, the increments in displacement are statistically independent, and then $\langle C_s(Y, Y^*)\rangle = 0$. This is the result expected for ordinary Brownian motion. For $H > 0.5$ past and future increments are positively correlated, this type of behavior is known as persistent. For $H < 0.5$ past and future increments are negatively correlated, this type of behavior is known as anti-persistent. In both cases $\langle C_s(Y, Y^*)\rangle \neq 0$.

In order to obtain the correlation coefficient between the photometric time series of the second half of our series $Y(t)$, and the theoretical $Y^*(t)$, we applied Sugihara and May methodology. We correlated $Y^*(t)$, obtained from the series corresponding to the creep process, $X(t)$, with $Y(t)$ which is the second half, for the different steps increments $\boldsymbol{s}$. For further details, see Refs. [11,24].

4. Results and discussion

This is an active work, trying to use time series analysis for practical applications. Understanding a biological system's behavior and how it is altered under pathological conditions is a promising way of diagnosis. Specifically, we have linked photometrically recorded time series of erythrocytes under shear stress with growing embedding dimension E for the dynamical process and scale exponent, to be able to compare and understand the changes on two different erythrocytes populations: healthy donor samples and patients affected by AL.

The algorithms for calculating the quantifiers were developed in two different programming languages: R [25] and MATLAB [26], which are at disposal if required. Certainly, the use of a nonlinear quantifier is not intended to replace conventional analysis, but to provide further insights into the underlying RBCs deformation mechanisms.

The random behavior is, as one expect, unpredictable, thus the question of randomness in data series is more than a question of mixtures of determinism and randomness. Since noise is present in all physical measurements, determining if randomness is inherent in the system dynamics or in the measurement process is not always straightforward. Furthermore, the mechanisms through which AL could induce vascular damage are at the same time metabolic and mechanical.

By the very beginning, we applied to all the series the first differences $(x_{t+1} - x_t)$ in order to whiten the series, that is, to reduce the autocorrelation, and also to diminish any signals associated with simple cycles. In order to reconstruct the process dynamics we use the technique of delay coordinates suggested by Takens and co-workers, and the phase space dimension was chosen applying Abarbanel method of false nearest neighbors, explained in Section 3.3. Thus, we obtained the %FNN for seven different and increasing embedding dimensions. For all the samples it was found that when $E = 6$ the %FNN was less than 1%, and the system's attractor would be completely unfold. Thus, $E = 6$ was the chosen embedding dimension for our analysis. The results obtained are shown in Fig. 2.

In order to improve the results, we studied surrogates time series. In this case, surrogates are shuffled generated by dividing all the series of 3500 data points, in 100 series of 35 data consecutive points each, and concatenating them at random, to generate new and different time series with the same length. As a consequence, the number of surrogate data sets that can be generated is considerably increased, because any perturbation of the trial segments yields new surrogates time series. However, one should be careful, because if two different permutations move a given trial segment into the same location, the terms of the test statistic will be the same for both permutations. This effect has been avoided.

So, for testing the method and the proposed algorithm we contrasted it with all the time series of shuffle surrogates. This is a random process in which the values at each time are statistical independent from each other. The process has no memory; past values have no impact in subsequent values as it is expected on a shuffle surrogate (noisy) time series.

Fig. 3 shows the outputs from the Sugihara and May applied methodology. Results showed differences comparing samples without treatment (healthy controls) and samples with adult AL extracts incubated, mainly at the first five steps when control samples generated lower correlations than the incubated ones. However, some independence between the correlation and

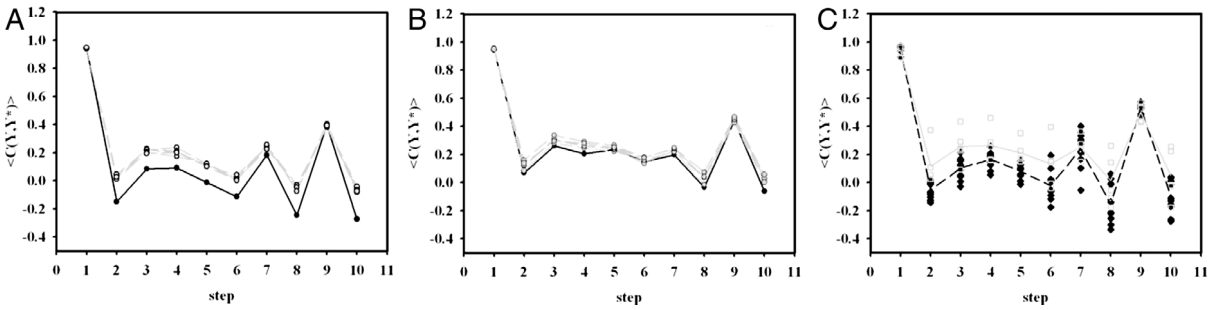

Fig. 3. Correlation coefficient versus step for: (A) Control RBCs (black) and average surrogates (gray). (B) RBCs incubated with adult *Ascaris lumbricoides* extracts (black) and average surrogates (gray). (C) Control RBCs (black) with their average (black dotted line) and RBCs incubated with adult *Ascaris lumbricoides* extracts (gray) with their average (gray dotted line).

Table 1
Mean Hurst exponent for all the populations.

Samples	Hurst ($s = 1$)	Hurst ($s = 2$)
Healthy controls	0.985 ± 0.009	0.46 ± 0.04
AL extracts incubated	0.98 ± 0.01	0.57 ± 0.06
Healthy control surrogates	0.981 ± 0.001	0.5 ± 0.1
AL extracts incubated surrogates	0.97 ± 0.04	0.6 ± 0.1

the step process could appear because we are dealing with uncorrelated additive noise. The accuracy of the prediction for healthy controls, as measured by $\langle C_s(Y, Y^*)\rangle$, shows no systematic dependence on $\boldsymbol{s}$, between experimental and theoretical ones. By contrast, for adult AL extracts incubated samples, the $\langle C_s(Y, Y^*)\rangle$ does not decrease with increasing $\boldsymbol{s}$, which is characteristic of a chaotic sequence.

Table 1 presents mean Hurst exponents for all the samples at $s = 1, 2$ steps increments. It is possible to infer, for $s = 2$, that on samples without treatment (healthy controls), it could be analyzed as an ordinary Brownian motion (i.e., H value around of 0.5), where statistical properties such as invariance or range are not related at all. On the other hand, on samples with adult AL extracts incubated, it would be a persistent fractional Brownian motion ($H > 0.5$), which is fractal in a statistical sense, that is, statistical properties are related over different time scales by way of a power law. In other words, the stress process gives us some special information of the relaxation one in a short time and the series exhibit a great sensitivity to initial conditions.

This study found that Hurst exponent changes when analyzing the RBC sample populations. In other words, there is such thing as healthy variability. A decrease in this variability could indicate a decrease in health, and variability can endow a system with flexibility and hence the ability to respond and adapt to environmental stressors [27]. Whether this variability is random or chaotic was a key in this study. Besides, enables the possibility of studying samples with AL extracts incubated with samples of healthy RBCs in terms of nonlinear dynamics. One of the hopes of the recent application of nonlinear dynamical methods to physiology is that introducing these new proposed quantifiers could help with the description of the different red cell networks that could put at stake the cytoplasm and membrane interactions. Moreover, the present results open the possibility of applying novel techniques based on photometrically recorded series from erythrocytes subjected to shear stress, for a quantitative characterization of the behavior of the system under study. Works in this direction, and also further studies with larger and well defined patient populations are in process in order to attain a better validation of the method.

5. Conclusions

Randomness and structural correlations are not totally independent aspects of the accompanying physical and biological description of the erythrocytes deformation. Ascertaining the degree of unpredictability and randomness of a dynamical biological system is not an automatically issue in the sense of allowing us the capture of the relationship between the components of the pertinent process. Moreover, maximal randomness as well as perfect order has no structural correlations. In between these two extremes a wide range of possible degrees of physical structures exists on the data that should be found in the behavior of the probability distribution.

This is an active work, trying to use time series analysis for practical applications, this includes the identification of those erythrocytes from healthy individuals from those erythrocytes incubated with adult AL extracts and allow not only the understanding of erythrocyte behavior of patients with severe anomalies and early diagnosis but also allow classification of the disease from the point of view of nonlinear dynamics.

In this work it was first proved the consistence of the employed methodology through the analysis of shuffle surrogates obtained from all the recorded time series. Then, it was applied the method for the erythrocytes samples without treatment

(healthy controls), resulting also ordinary Brownian motion. Finally we obtained the correlation coefficient for the series of adult AL extracts incubated erythrocytes, and in those cases the results have shown that the correlation coefficient for the firsts steps of the process, increased when increasing the steps of the process. Those erythrocytes in the adult AL extracts incubated samples have lost the viscoelastic properties, proving there is some fractal like underlying behavior.

Several hemorheological variables could influence and produce an impaired erythrocyte deformability determining an increased flow resistance in the microcirculation. Once we can predict the future, it is natural to try to control that future, in order to guide the system to a preferred state or keep it away from undesired states.

These basic goals of understand, predict and control are closely related to the practical clinical goals of diagnosis and treatment, which underlie much of the rationale for research into physiological systems.

References

[1] C.M. Peterson, R.L. Jones, R.J. Koenig, E.T. Melvin, M.L. Lehrman, Ann. Intern. Med. 86 (1993) 425.
[2] C. Brown, H. Ghali, Z. Zhao, L. Thomas, E. Friedman, Kidney Int. 67 (2005) 295.
[3] M. Szelachowska, W. Schaefer, A.F. Gries, I. Kinalska, Endocrinol. Pology 43 (1992) 23.
[4] A. Lapolla, C. Gerhardiger, M. Dal Frá, A. Franchin, D. Fedele, G. Crepaldi, Clin. Hemorheol. 11 (5) (1991) 405.
[5] F. Torregiani, M. Umansky-Zeverin, B. Riquelme, R. Rasia, Clin. Hemorheol. 15 (1995) 687.
[6] P. Ponce de león, J. Valverde, B. Riquelme, Rev. Soc. Ven. Microb. 32 (2012) 62.
[7] P. Ponce de León, N. Lebensohn, P. Foresto, J. Valverde, Rev. Inst. Med. Trop. Sao Paulo 51 (2009) 219.
[8] P. Ponce de León, K. Juarez Matamoros, C. Biondi, J. Valverde, Rev. Cuba. Med. Trop. 63 (2011) 87.
[9] M. Lupo, A.J. Leguto, S.A. Bortolato, A.M. Korol, Ain Shams Eng. J. (2016). http://dx.doi.org/10.1016/j.asej.2016.12.004.
[10] H.D.I. Abarbanel, R. Brown, J.J. Sidorowich, L.S. Tsimring, Rev. Modern Phys. 65 (1993) 1331.
[11] G. Sugihara, R. May, Nature 344 (1990) 734.
[12] B. Riquelme, F. Foresto, M. D'Arrigo, J. Valverde, R. Rasia, J. Biochem. Biophys. Methods 62 (2005) 131.
[13] Guidelines for measurements of blood viscosity and erythrocyte deformability, Clin. Hemorheol. Microcirc. 6 (1996) 439 International Committee of Standardization Haemathology (Expert Panel on Blood Rheology).
[14] H. Castellini, B. Riquelme, P. Foresto, J. Valverde. Anal. AFA 20 (2009) 219–223.
[15] B. Albea, A. Marenzana, H. Castellini, B. Riquelme, Biochim. Clin. 37 (2013) S437.
[16] R. Rasia, Clin. Hemorheol. 15 (1995) 177.
[17] R. Rasia, P. Porta, M. García Rosasco, Rev. Sci. Instrum. 57 (1986) 33.
[18] A. Korol, P. Foresto, O. Rosso, Physica A 386 (2007) 770.
[19] A. Korol, R. Rasia, Chaos 13 (2003) 87.
[20] A. Korol, J. Valverde, R. Rasia, Exp. Mech. 42 (2002) 172.
[21] J. Theiler, S. Eubank, A. Longtin, B. Galdrikian, J. Farmer, Physica D 58 (1992) 77.
[22] F. Takens, Detecting strange attractors in turbulence, in: D. Rand, L.S. Young (Eds.), Dynamical Systems and Turbulence, in: Lecture Notes in Mathematics, Springer-Verlag, Heidelberg, 1981, pp. 366–381.
[23] I. Simonsen, Physica A 322 (2003) 597.
[24] J. Feder, Fractals, Plenum Press, New York, 1988.
[25] R Core Team, R: A Language and Environment for Statistical Computing, R Foundation for Statistical Computing, Vienna, Austria, 2016. (http://www.R-project.org/).
[26] MATLAB. The Mathworks Inc., Natick, Massachusetts, USA, 2013.
[27] P. Bak, How Nature Works, Springer-Verlag, New York, 1996.